Effect of interactions among individuals on the chemotaxis behaviours of *Caenorhabditis elegans.*

Authors: Toshiki Yoshimizu[1, 3], Hisashi Shidara[1, 3], Keita Ashida[1], Kohji Hotta[1] and Kotaro Oka[1, 2*]

1. Department of Biosciences and Informatics, Faculty of Science and Technology, Keio University, Yokohama, Kanagawa, 223-8522, Japan

2. Graduate Institute of Medicine, College of Medicine, Kaohsiung Medical University, Taiwan

3. Equal contribution

*Correspondence: oka@bio.keio.ac.jp

Keyword

C. elegans, collective behaviour, olfactory, behaviour, pheromone

Summary statement

By comparing isolated worms with oness in a population, we revealed that chemotactic behaviours of *Caenorhabditis elegans* in the population is modulated by pheromones, leading changes in collective behaviours.

Abstract

In many species, individual social animals interact with others in their group and change their collective behaviours. Meanwhile, for the solitary nematode *Caenorhabditis elegans* strain, N2, previous research suggests that individuals can change the behaviour of other worms *via* pheromones and mechanosensory interactions. Pheromones, especially, affect foraging behaviour, so that the chemotactic behaviours of individuals in a group (population) can be modulated by interactions with other individuals in the population. To investigate this, we directly compared the chemotactic behaviours of isolated (single) worms with those of individual animals within a population. Here, we showed that worms approached an odour source in a distinct manner depending on whether they were in the single or population condition. From analysis of behaviours with the N2 and a pheromone-production-defective mutant, the pirouette strategy was modulated by interaction of worms *via* pheromones. Therefore, we clarified that pheromones play an important role in the characteristic collective behaviours seen in the population condition.

Introduction

Individual animals interact with others in their group, leading to changes in collective behaviour. The collective behaviours of swarming ants, schooling fish and flocking birds in groups of social animals have been previously studied (Sumpter, 2006; Visscher, 2007; Couzin, 2009; Herbert-Read, 2016). Recently, *Drosophila melanogaster,* which is classified as a solitary species, was also shown to exhibit collective behaviours driven by mechanosensory interactions (Ramdya et al., 2015). Although the laboratory nematode *Caenorhabditis elegans* strain, N2, which has acquired a gain-of-function in the *npr-1* neuropeptide receptor is a solitary species (de Bono and Bargmann, 1998; Rockman and Kruglyak, 2009; Weber et al., 2010), population density regulates reproductive development and dauer (*C. elegans* larvae arrested at the second moult) formation *via* pheromones (Ludewig and Schroeder, 2013). Thus, like *Drosophila*, worms may affect each other's behaviours. In fact, pheromone signalling affects olfactory adaptation (Yamada et al., 2010), and some ascaroside pheromones regulate exploratory foraging in *C. elegans* (Greene et al., 2016a; Greene et al., 2016b). Moreover, physical contact has been shown to influence collective behaviours; swimming behaviour synchronizes as two worms approach each other (Yuan et al., 2014). Taken together, chemotactic behaviours in populations are inevitably represented as collective behaviours, which include crucial roles for competitively approaching resources. As discussed above, although factors that have an important influence on collective behaviours in *C. elegans* have been identified, there has been no research directly comparing the chemotactic behaviours of isolated worms with those of individual animals from populations.

Several studies on *C. elegans* describe chemotactic behaviours in single animals (Pierce-Shimomura et al., 1999; Iino and Yoshida, 2009; Wakabayashi et al., 2015; Yamazoe-Umemoto et al., 2015), namely the pirouette and weathervane strategies. In the pirouette strategy, worms show directional changes with sharp turns, 'pirouettes', when they detect a negative temporal change in the odour concentration ($dC/dt < 0$) (Pierce-Shimomura et al., 1999). In the weathervane strategy, animals

gradually move to higher concentration regions (Iino and Yoshida, 2009). Although these methods have mainly been used to investigate the behaviour of isolated worms, it is unclear whether the behaviour of *C. elegans* differs depending on interactions with other worms.

Here, we compared the behaviour of *C. elegans* in a chemotaxis assay under different collective conditions. To investigate the trajectories under each condition, we showed that worms approached an odour source in different manners based on their interaction with other worms. In addition, by using mutants with defective production of pheromones, we demonstrated that pheromones were necessary for the collective behaviour shown in the population condition.

Materials and methods

Strains

All strains were cultured at 20°C on nematode growth medium (NGM) plates with *Escherichia coli* OP50 (Brenner, 1974). The strains were hermaphrodite N2, which is used as a wild-type in the laboratory, and hermaphrodite *daf-22* (m130) II mutants, which is defective in producing some kinds of pheromones, ascarosides.

Chemotaxis assay

We designed three conditions for the chemotaxis assay: single, population and paired (Fig. 1A, B). The assay plate consisted of 8 ml of 1.8% agar, 1 mM $CaCl_2$, 1 mM $MgSO_4$ and 5 mM KH_2PO_4 in a 10-cm petri dish (Thermo Fisher Scientific, Waltham, Massachusetts, U.S.A.). In all experiments, some worms were moved into S-basal buffer in a microtube with a sterilized platinum wire, and were washed. Then, we transferred all of the worms to an assay plate with buffer to enable picking each worm in the subsequent procedure easily. For each assay, eight worms in total were moved to start points on another assay plate where 2.5 µl (single and paired) or 4 µl (population) of distilled water

(DW) was spotted in advance (Fig. 1B). The numbers of animals in each spot were as follows: single, one; population, eight; paired, two. Any excess DW was immediately removed with Kimwipes. Then, 1 µl of 10^{-2} dilution of isoamyl alcohol (IAA) in ethanol (EtOH) was spotted, while 1 µl of EtOH was also spotted on the other side of the plate. On each spot, 500 mM of sodium azide (an anesthesia) was applied in advance so that animals are restrained after reaching the odour spot. The total time for chemotaxis assay was 30 minutes.

Image acquisition and analysis

We captured images (1080×1080 pixels, 0.09 mm/pixel) with a web camera (HD Pro Webcam C920, Logitech, Lausanne, Switzerland) fixed on a stand, every second for 30 minutes using a custom-made program written in MATLAB 2016a (MathWorks, Natick, Massachusetts, U.S.A.). An assay plate was set on an A4 sized LED light source (1-2785-11, AS ONE Corporation, Osaka, Japan) with the lid on the bottom. To ensure that the figures of transparent animals were clear in dark field, a sheet of black paper was placed on the lid.

For analysis, we initially obtained the tracks of the animals using a modified parallel worm tracker in MATLAB (Ramot et al., 2008). In the original program, the tracks of each worm were sometimes distorted due to noise or collisions of the animals. Here, we aimed to track the trajectory of each animal from start to finish, so we complemented some parts of the trajectories and combined fragments of trajectories manually. Instances where worms rarely moved from their start point were discarded from further analyses. The proportion of the animals (the number of worms immobilizing / the number of total animal) is as follows: N2, single 3/96, population 0/96, paired 1/96; *daf-22* mutants, single 6/96, population 1/96, paired 2/96. In addition, if worms arrived at the high odour concentration area, their subsequent trajectories were removed from the data set because the animals were immobilized by sodium azide. For worms that reached the edge of plates, the trajectories data before arrival at the

edge was used for the analysis because most animals climbed the sidewall after that. Before the analysis, x and y positions were respectively smoothed by a median filter with every five-time point (5 s). Distances between individual worms were calculated as the mean Euclidian distance from each worm to all other worms at a particular time. For the single and paired conditions, the distances were calculated after the start points of each animal were translocated to the centre of the plate and rotated (Fig. S1), because the starting points of individual animals were different in these conditions without such translocation and rotation. In brief, the distances in the single and paired conditions are estimated based on the assumption that worms had started from the centre like ones in the population condition. The chemotaxis index was calculated as follows: ((the number of animals within a radius of 1 cm of the odour spot) – (the number of animals at the other area)) / (the total number of animals on the plate).

The behaviours of worms are so simple that the trajectories were analysed with the conventional ways (Pierce-Shimomura et al., 1999; Iino and Yoshida, 2009; Wakabayashi et al., 2015; Yamazoe-Umemoto et al., 2015). Behaviours were categorized into three groups: run, pirouette and immobilized. The following analysis of pirouette behaviours are referred in the previous research (Pierce-Shimomura et al., 1999). The pirouette behaviour includes sharp turns and subsequent short-term migrations. In our experiments, sharp turns were defined as instances where the absolute turning rate ($|d\theta|/dt$) was over 90°. Angle changes ($d\theta$) were differences in direction before and after specific time points. Using this criterion, behaviours were classified as sharp turns and migrations. The distribution of migrations was fitted by the sum of two exponentials, to give the critical migration duration t_{crit} (Pierce-Shimomura et al., 1999). According to our preliminary experiment, the duration was calculated to be t_{crit} = 12.92 s (data not shown). Therefore, animals that had durations of less than t_{crit} and sharp turns were designated as having performed a pirouette, while ones for which the migration duration was longer, were classified as run behaviour. In addition, when worm velocity was < 0.01 mm/s in a half of ten sequential time points, worms were designated as immobilized.

To analyse the pirouette initiation rate, we calculated it as follows. First, pirouette initiation rates were calculated for each specific term. Data were fitted with the sigmoid function:

$$P_{pirouette} = \frac{\beta}{1+e^{\alpha \times \frac{dC}{dt}}} + \delta, \quad (1)$$

where $P_{pirouette}$ is the pirouette initiation rate against the time derivative of the odour concentration (dC/dt), and α, β and δ were parameters. These parameters were determined by curve fitting with non-linear least squares methods (MATLAB 2016a, MATLAB fit function with the NonlinearLeastSquares option). To analyse the effect of collisions between worms, we calculated the cosine of the directional vectors before and after a collision and the vectors to odour source (Fig. S3B), which was defined as direction values and attracted values. In this case, a collision was designated if worms were less than 0.5 mm from one another. The directional vectors used here were the same ones used to calculate the curving rates, described below.

To analyse the weathervane strategy, we calculated the curving rate as previously described (Iino and Yoshida, 2009). The concentration gradient orthogonal to the worms' direction was obtained as follows. For each time point, we first identified the worm's direction and calculated the concentration gradient orthogonal to it. For analysis of worms crossing trails, we decided the points when worms crossed the trails with semi-automated program written with MATLAB. To obtain the probability of pirouettes occurred by 10 s after worms crossed trail, the total number of pirouettes was divided by the total number of passing trails. The binominal test for this probability was conducted as follows. First, we examined the number of pirouettes occurred by 10 s from specific time points sampled randomly. The number of time points chose in each worm was the mean number of the worms crossing the trails in the experimental data. Then, we repeated this process 1000 times and obtained the mean probability of pirouettes by 10 s after random time points, as hypothesized probability. The parameters used in binominal test and the results were in Table S2. The directions before and after worms crossed the trails were calculated from every five-time point (5 s) before and after the events

(Fig. S5C, E). The direction of the trails was calculated from the trajectories of the trails. All statistical tests were performed in R (version 3.4.1, exactRankTests and kSamples libraries) except for regression analysis. The regression analysis conducted by Excel 2016 (Microsoft, Washington, U.S.A.).

Numerical estimation of odour gradient

To estimate odour distribution on agar surface where worms moved, we used a numerical simulation written in C++. The concentration of IAA and EtOH was calculated with a three-dimensional diffusion equation:

$$\frac{\partial C}{\partial t} = D\nabla^2 C. \qquad (2)$$

The equation was solved with the second-order central difference method (Press et al., 1992) for 30 min. The diffusion coefficients in the air were D_{EtOH} = 0.123 cm^2·s^{-1} and D_{IAA} = 0.0692 cm^2·s^{-1} (Yaws, 2009a; Yaws, 2009b). The boundary condition for the gas-surface at specific odour spots was determined using methods described previously (Yamazoe-Umemoto et al., 2015) (Personal communication, Y. Iwasaki):

$$-D\frac{\partial C}{\partial z} = \frac{E}{M}\left(\gamma(t)\chi(t) - \frac{C}{C_{sat}}\right). \qquad (3)$$

The evaporation rates per unit time and unit area were E_{EtOH} = 1.98×10^{-11} g·cm^{-2}·s^{-1} and E_{IAA} = 0.127×10^{-11} g·cm^{-2}·s^{-1}, and the saturation concentrations were $C_{satEtOH}$ = 3.19 mM and C_{satIAA} = 34.5 μM (ASTM D3539-87, 2004; Nylén and Sunderland, 1965).

The activity coefficients were γ_{EtOH} = γ_{IAA} = 1 (Ramsbotham, 1980). $\chi(t)$ was the molar fraction, and M was the molecular weight (EtOH, 46.07 g·mol^{-1}; IAA, 88.148 g·mol^{-1}). The initial radius of the odour spot was 6 mm. The Neumann boundary condition was used for the other surfaces including the wall and lid. The radius of the plate was 45 mm, and the height was 10 mm. After simulation, spline interpolation (MATLAB fit function with the cubicinterp option) was used to

calculate the odour concentration at the worms' location because the spatial mesh of the simulation was coarser than the measurement.

Results

Interactions between individuals affect the trajectories of chemotaxis

To reveal whether interactions between worms affect chemotaxis, we examined chemotaxis with worms under two conditions: single and population. For the single condition, one worm was set at each starting point with even spacing and the same estimated odour concentration, while for the population condition, eight worms commenced chemotaxis from the same point (Fig. 1B). Compared with worms in the population condition, those in the single condition were likely to move to the odour source directly (Fig. 1C). In contrast, it appeared that worms in the population condition dispersed away from their neighbouring worms. To understand this quantitatively, we calculated the distances from each worm to the other worms. For the single and paired conditions (described below), the distances were estimated after the start point of each worm was transferred and superimposed to the centre of the plate (Fig. S1, see materials and methods). The distances between individual animals in the population condition increased more rapidly than those in the single condition in first 200 s (Fig. 1D), suggesting that the trajectories of chemotaxis differed between the single and population conditions.

Next, we examined whether the phenomenon described above could be caused by interactions between worms. To address this question, we used a paired condition in which two worms were set evenly at each starting point (Fig. 1B). In the paired condition, the trajectories also appeared to spread (Fig. 1C), and the distances between individual animals increased steeply, similar to the measurements in the population condition (Fig. 1D), suggesting that the same phenomenon observed in the population condition also occurred in the paired condition. Therefore, these results indicate that interactions between two worms are an important factor for affecting chemotactic behaviours.

Although worms in the population and paired conditions did not appeared to move the odour source directly around the start points compared with the single condition, the movement distances did not differ between conditions (Fig. 1E). Similarly, the attraction to odour in 30 minutes was the same for all conditions (Fig. 1G). In contrast, worms in single condition moved slower than ones in the population condition (Fig. 1F). Based on these results, behaviours barely differed between conditions, but interactions between two worms appeared to alter their approach trajectories towards the odorant. This suggests that interactions between two or more worms can change the behavioural process used to reach the odour source.

Interactions affect pirouette strategies

Previous research has revealed that single worms use pirouettes (Pierce-Shimomura et al., 1999) and weathervane strategies (Iino and Yoshida, 2009) to approach attractants. Pirouettes, which include sharp turns and subsequent short-migrations, allow worms to drastically change direction towards an odour source. Because worms in the population and paired conditions required large directional changes to move to the odour source, pirouettes may play an important role in interactions between worms. Compared with the single condition, the probabilities of pirouettes in the population and paired conditions (collective conditions) differed, but the population and paired conditions did not show any common tendencies (Figs. 1H, S2). To investigate this further, we evaluated the distribution of the time derivatives of the odour concentration (dC/dt) at pirouette initiation (Fig. 2), as the occurrence of pirouettes depends on dC/dt (Pierce-Shimomura et al., 1999). The cumulative probability distribution in the single condition became steeper than that found for the collective conditions (Fig. 2B, left and centre), and the distributions in the population and paired conditions showed a similar trend (Fig. 2B, right). These results indicate that worms in the single condition initiated pirouettes for smaller changes in odour concentration.

Pheromones are crucial for chemotaxis with interaction

According to the results of the collective conditions (Figs. 1D, 2B), worms in the population and paired conditions showed similar trends in behaviour. Remarkably, worms appeared to avoid each other in population and paired condition (Fig. 1D); thus, interactions between two or more worms could change their chemotactic behaviours towards odorants. The conceivable reason is pheromone signals and physical contacts. Thus, we investigated whether pheromones altered behaviour between the single and paired conditions. Here, we used the *daf-22* mutant in which a kind of pheromones, ascarosides, were not produced (Golden and Riddle, 1985; Jeong et al., 2005; Butcher et al., 2007; Pungaliya et al., 2009). As expected, *daf-22* mutants in the paired condition showed the similar tendency in chemotactic behaviours of ones in the single condition (Fig. 3A). The difference between N2 in the single and paired conditions (Fig. 2) disappeared by lack of pheromones (Fig. 3G, H), so that pheromones modulate the initiation of pirouettes by given stimuli. Meanwhile, the results of the population condition were not our expectation. Compared with the other conditions, *daf-22* mutants spread out from the start point (Fig. 3A) and the parameters of chemotactic behaviour were significantly different (Fig. 3B-D). Remarkably, *daf-22* mutants in the population condition collided each other much more times than the other conditions including N2 (Figs. 3F, S3A). This suggested that the cause that the tendency of *daf-22* mutants in the population was different from ones in the single and paired condition would be physical contacts. Actually, the slope of *daf-22* in population appeared to shift left and the inflection point was not around zero in *dC/dt*, suggesting that the physical contact drove pirouettes regardless of odour concentration. Taken together, interactions between individual worms *via* pheromones change chemotactic behaviour, decrease the temporal change of odour concentration in initiation of pirouettes.

As shown above, excessive physical contacts also increase frequency of pirouettes, leading

the change of chemotaxis. To investigate other effects of physical contact in the other conditions, we evaluated behaviour before and after collision (Figs. S3, S4). For N2, worms in the population condition collided more frequently than those in the other conditions (Fig. S3A). To understand whether physical contacts change behaviours, the running directions of worms before and after collisions to odour source were calculated by defining the cosine of the running direction as the direction value (Fig. S3B; see materials and methods). If this value is close to +1, worms do not change their direction before and after collisions. In all conditions, over a half of collisions showed close to +1 (Fig. S3C), suggesting that worms did not change their direction after physical contacts. In addition, we examined whether worms move to better towards after collisions (Fig. S3D, E). In all conditions, attracted values were uniformly distributed (Fig. S3D) and *dC*/*dt* before and after contacts had weak correlation (Fig. S3E, Table S1). For *daf-22* mutant, the same result appeared (Fig. S4). Taken together, although physical contacts increase the pirouette behaviour, they rarely affect chemotactic behaviours.

Crossing trails do not affect behaviours in chemotaxis.

Animals like ants crossing trails change their behaviours with cues left by others (Sumpter, 2006; Steck, 2012). In our experiments, worms crossed trails at many times (Fig. S5A). Thus, we examine whether crossing trails affect chemotaxis in *C. elegans* as well as other species. For all conditions, the probability of pirouettes occurring by 10 s after worms crossed trails was small (Fig. S5B). To examine whether crossing trails triggered pirouettes, we conducted the binominal test for each condition (Table S2, see materials and methods). The probability for each condition was not significantly different from the probability estimated from randomly-selected time points. Therefore, crossing trails do not affect the pirouette behaviour. Then, to investigate whether worms changed their direction after crossing, we compared the angles against the direction of trails (Fig. S5C). The relationships of the direction between before and after crossing had strong positive correlations (Fig. S5D, Table S1), suggesting

that worms did not change their direction over trails. The direction did not change depending on the worms' direction against the odour source, either (Fig. S5E, F). Therefore, crossing trails do not affect chemotactic behaviour in *C. elegans*.

Discussion

Previous research has suggested that chemotactic behaviours can be represented as collective behaviours due to the interactions between individual worms. To understand such interactions, we examined chemotaxis under three conditions: single, population and paired. Based on the trajectories to the odour source, worms in the population and paired conditions displayed different behaviours from those in the single condition. Further investigation showed that the temporal changes of odour concentration in initiating pirouettes became lower when worms interacted with each other. Finally, experiments conducted with the *daf-22* mutant suggested that this phenomenon resulted from the interactions between individual animals *via* pheromones.

Thus far, analyses of behaviour in chemotaxis have been performed on single worms. Here, we revealed differences in the behaviour of *C. elegans* relative to the collective conditions. From the experiments with the *daf-22* mutant, we revealed that the response to temporal change of odour concentration driving pirouettes was altered by pheromones. This could explain why worms in the population and paired conditions left from each other (Fig. 1D). If pirouettes are driven by large temporal change in odour concentration, worms do not initiate pirouette behaviours until they approach odour source. Therefore, the timing of the movements of worms in the population and paired conditions were delayed, leading to greater spread in their trajectories. This may prevent many worms from approaching attractants at the same time. The same role of the pheromones for food exploration was reported (Greene et al., 2016a). In addition, other factors may regulate behaviours in populations. Although the excessive physical contact change chemotactic behaviours by increasing the pirouettes

(Fig. 3), the physical contact itself did not seem to affect the phenomenon remarkably (Figs. S3, 4).

The different causes triggering pirouette behaviours seemed that the analysis of pirouettes and odour concentration (Figs. 2, 3G, H) was perturbed because worms could use pirouettes to avoid each other. We could not completely exclude the disturbance from the analysis, but our results supported our conclusion. First, the character of pirouettes in our experiments was the same compared with the previous research (Pierce-Shimomura et al., 1999) (Fig. S2). Pirouettes were triggered when *dC/dt* got negative, suggesting the pirouettes occurred depending on change in odour concentration. Second, if worms avoid each other, they have to detect others by physical contacts or pheromones. Thus, the physical contacts could be a main cause triggering pirouettes independently of the change in odour concentration. However, for the results except for *daf-22* in the population condition, worms collided others less than twice (Figs. 3F, S3A). These collisions are so small that the influence is little. Meanwhile, the case of the *daf-22* mutant in the population condition meant that pirouettes were triggered independently of odour. The number of physical contacts in the condition was large (Fig. 3F), and the slope of cumulative probability shifted to left (Fig. 3H). These results would rather indicate that the analysis of pirouettes and odour concentration was perturbed. Although it is not revealed whether the pheromones themselves trigger pirouettes to avoid each other, as mentioned above (Fig. S2), the effect is probably little. Taken together, for the results except for one of *daf-22* in the population, the pheromone modulates the initiation of pirouettes depending on the change in the odour concentration, supporting our conclusion.

The regulation *via* pheromones changed the initiation rate of pirouettes in response to *dC/dt*. Pirouettes occurred when the time derivative of the odour concentration became negative (Pierce-Shimomura et al., 1999). In our results, the modulation was particularly observed when *dC/dt* was negative (Fig. S2). As well as the pirouette strategy, the weathervane strategy is important for migration to the odour source. Our results did not show that this strategy altered between the single

and collective conditions (Fig. S6). Although we concluded that the weathervane strategy was not affected in collective worms, our results could not exclude it as a cause of behaviour changes completely. If worms exhibited the weathervane strategy, the curving rate would increase against the vertical gradient along to direction of animals. However, N2 strain did not display this trend (Fig. S6A). Thus, the influence of the weathervane strategy could not be observed in our experimental setup.

Interactions between two worms changed the initiation of pirouettes and induced collective behaviours. So far, research on collective behaviours has been performed on social animals. Our results show that the solitary *C. elegans* can be used as an experimental model along with other solitary species like *Drosophila* (Ramdya et al., 2015). These animals have advantages for genetic experimental approaches (Ramdya et al., 2017). In addition, tracking systems, which are important for studies on collective behaviours (Herbert-Read, 2016), have already been developed for *C. elegans* (Yemini et al., 2011; Husson et al., 2013); thus, the species can contribute to research on collective behaviour.

Acknowledgements

All strains were given by the CGC, which is funded by NIH Office of Research Infrastructure Programs (P40 OD010440). We thank Dr. Yuishi Iwasaki for giving us information about the computer simulation.

Competing interests.

We have no competing interests.

Authors' Contributions.

T.Y. performed all experiments and made figures. H.S. wrote the most main manuscript text and K.A. performed the computer simulation and wrote the text about the computer simulation in materials and methods. K.O. and K.H. supervised this research. All authors designed the experiments and reviewed the manuscript.

Funding

This research was supported by Japan Society for the Promotion of Science (JSPS) Grant-in-Aid for JSPS Fellows Grant Number 14J06037 (H.S.).

References

ASTM D3539-87 (2004). Standard Test Methods for Evaporation Rates of Volatile Liquids by Shell Thin-Film Evaporometer. *Am. Soc. Test. Mater.*

Brenner, S. (1974). The genetics of *Caenorhabditis elegans*. *Genetics* **77**, 71–94.

Butcher, R. A., Fujita, M., Schroeder, F. C. and Clardy, J. (2007). Small-molecule pheromones that control dauer development in *Caenorhabditis elegans*. *Nat. Chem. Biol.* 3, 420–2.

Couzin, I. D. (2009). Collective cognition in animal groups. *Trends Cogn. Sci.* **13**, 36–43.

de Bono, M. and Bargmann, C. I. (1998). Natural variation in a neuropeptide Y receptor homolog modifies social behavior and food response in *C. elegans*. *Cell* **94**, 679–89.

Golden, J. W. and Riddle, D. L. (1985). A gene affecting production of the *Caenorhabditis elegans* dauer-inducing pheromone. *Mol. Gen. Genet.* **198**, 534–6.

Greene, J. S., Brown, M., Dobosiewicz, M., Ishida, I. G., Macosko, E. Z., Zhang, X., Butcher, R. A., Cline, D. J., McGrath, P. T. and Bargmann, C. I. (2016a). Balancing selection shapes density-dependent foraging behaviour. *Nature* **539**, 254–258.

Greene, J. S., Dobosiewicz, M., Butcher, R. A., McGrath, P. T. and Bargmann, C. I. (2016b). Regulatory changes in two chemoreceptor genes contribute to a *Caenorhabditis elegans* QTL for foraging behavior. *eLife* **5**,.

Herbert-Read, J. E. (2016). Understanding how animal groups achieve coordinated movement. *J. Exp. Biol.* **219**, 2971–2983.

Husson, S. J., Costa, W. S., Schmitt, C. and Gottschalk, A. (2013). Keeping track of worm trackers. *WormBook* 1–17.

Iino, Y. and Yoshida, K. (2009). Parallel use of two behavioral mechanisms for chemotaxis in *Caenorhabditis elegans*. *J. Neurosci.* **29**, 5370–80.

Jeong, P.-Y., Jung, M., Yim, Y.-H., Kim, H., Park, M., Hong, E., Lee, W., Kim, Y. H., Kim, K. and Paik, Y.-K. (2005). Chemical structure and biological activity of the *Caenorhabditis elegans* dauer-inducing pheromone. *Nature* **433**, 541–5.

Ludewig, A. H. and Schroeder, F. C. (2013). Ascaroside signaling in *C. elegans*. *WormBook* 1–22.

Nylén, P. and Sunderland, E. (1965). *Modern Surface Coatings: a textbook of the chemistry and technology of paints, varnishes, and lacquers*. NY, USA: Interscience Publishers.

Pierce-Shimomura, J. T., Morse, T. M. and Lockery, S. R. (1999). The fundamental role of pirouettes in *Caenorhabditis elegans* chemotaxis. *J. Neurosci.* **19**, 9557–69.

Press, W. H., Teukolsky, S. A., Vetterling, W. T. and Flannery, B. P. (1992). *Numerical Recipes in C (2nd Ed.): The Art of Scientific Computing*. New York, NY, USA: Cambridge University Press.

Pungaliya, C., Srinivasan, J., Fox, B. W., Malik, R. U., Ludewig, A. H., Sternberg, P. W. and Schroeder, F. C. (2009). A shortcut to identifying small molecule signals that regulate behavior and development in *Caenorhabditis elegans*. *Proc. Natl. Acad. Sci. U. S. A.* **106**, 7708–13.

Ramdya, P., Lichocki, P., Cruchet, S., Frisch, L., Tse, W., Floreano, D. and Benton, R. (2015). Mechanosensory interactions drive collective behaviour in *Drosophila*. *Nature* **519**, 233–6.

Ramdya, P., Schneider, J. and Levine, J. D. (2017). The neurogenetics of group behavior in *Drosophila melanogaster*. *J. Exp. Biol.* **220**, 35–41.

Ramot, D., Johnson, B. E., Berry, T. L., Carnell, L. and Goodman, M. B. (2008). The Parallel Worm Tracker: a platform for measuring average speed and drug-induced paralysis in nematodes. *PLoS One* **3**, e2208.

Ramsbotham, J. (1980). Solvent formulation for surface coatings. *Prog. Org. Coatings* **8**, 113–141.

Rockman, M. V and Kruglyak, L. (2009). Recombinational landscape and population genomics of *Caenorhabditis elegans*. *PLoS Genet*. **5**, e1000419.

Steck, K. (2012). Just follow your nose: homing by olfactory cues in ants. *Curr. Opin. Neurobiol.* **22**, 231–5.

Sumpter, D. J. T. (2006). The principles of collective animal behaviour. *Philos. Trans. R. Soc. Lond. B. Biol. Sci.* **361**, 5–22.

Visscher, P. K. (2007). Group decision making in nest-site selection among social insects. *Annu. Rev. Entomol.* **52**, 255–75.

Wakabayashi, T., Sakata, K., Togashi, T., Itoi, H., Shinohe, S., Watanabe, M. and Shingai, R. (2015). Navigational choice between reversal and curve during acidic pH avoidance behavior in *Caenorhabditis elegans*. *BMC Neurosci.* **16**, 79.

Weber, K. P., De, S., Kozarewa, I., Turner, D. J., Babu, M. M. and de Bono, M. (2010). Whole genome sequencing highlights genetic changes associated with laboratory domestication of *C. elegans*. *PLoS One* **5**, e13922.

Yamada, K., Hirotsu, T., Matsuki, M., Butcher, R. A., Tomioka, M., Ishihara, T., Clardy, J., Kunitomo, H. and Iino, Y. (2010). Olfactory plasticity is regulated by pheromonal signaling in *Caenorhabditis elegans*. *Science* **329**, 1647–50.

Yamazoe-Umemoto, A., Fujita, K., Iino, Y., Iwasaki, Y. and Kimura, K. D. (2015). Modulation of different behavioral components by neuropeptide and dopamine signalings in non-associative odor learning of *Caenorhabditis elegans*. *Neurosci. Res.* **99**, 22–33.

Yaws, C. L. (2009a). Diffusion Coefficient in Air – Inorganic Compounds. In *Transport Properties of Chemicals and Hydrocarbons*, pp. 497–501. Elsevier.

Yaws, C. L. (2009b). Diffusion Coefficient in Air – Organic Compounds. In *Transport Properties of Chemicals and Hydrocarbons*, pp. 407–496. Elsevier.

Yemini, E., Kerr, R. A. and Schafer, W. R. (2011). Tracking movement behavior of multiple worms on food. *Cold Spring Harb. Protoc.* **2011**, 1483–7.

Yuan, J., Raizen, D. M. and Bau, H. H. (2014). Gait synchronization in *Caenorhabditis elegans*. *Proc. Natl. Acad. Sci. U. S. A.* **111**, 6865–70.

Figures

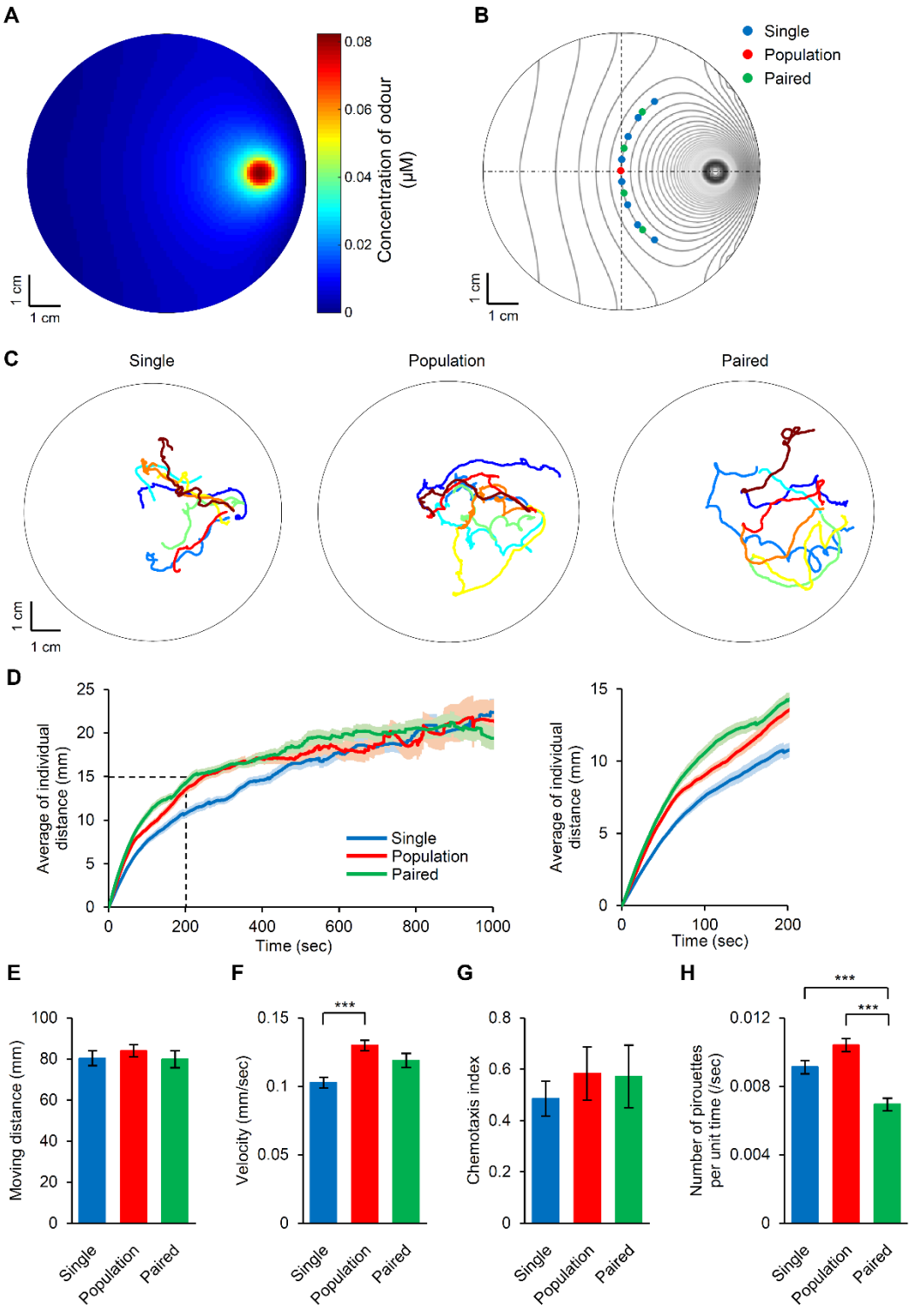

Fig. 1. The chemotaxis behaviour of worms in the collective conditions. (A) Simulated odour concentration in the assay plate. (B) Start positions in each condition. Each point indicates the place where worms were spotted (see materials and methods). Contour lines show the odour concentration. Blue, single; red, population; green, paired. (C) Representative results for each condition. Colours indicate each animal. (D) Average distances between individual worms. Each trace indicates the average distance between neighbouring worms. Shading in the graphs shows the standard error of the mean (s.e.m.). The right graph is an enlarged image of the dotted box in the left graph. (E-H) Mean of the moving distance (E), velocity (F), chemotaxis index (G), and number of pirouettes per unit time (H). Error bars indicate s.e.m. (N = 12, n = 93, 96 and 95 respectively; (E, H), Mann-Whitney *U* test with Bonferroni correction; (F, G), Student's *t*-test with Bonferroni correction; ***p < 0.001 significant difference).

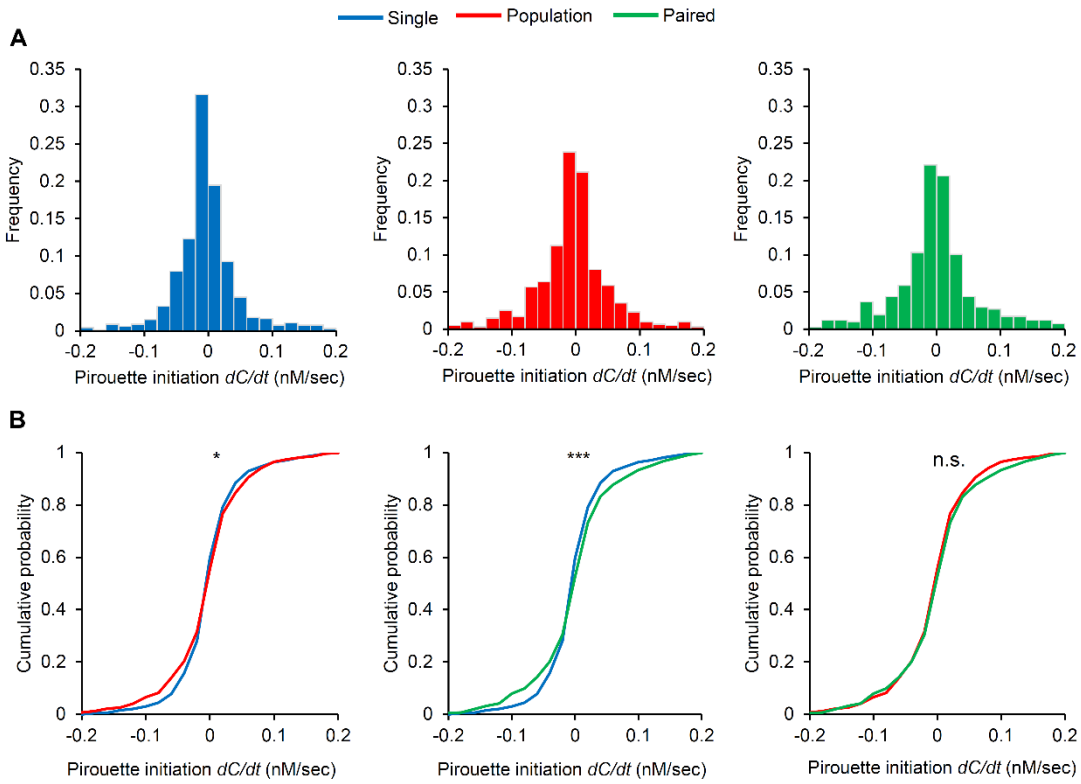

Fig. 2. Time derivative of the odour concentration eliciting pirouette behaviours. (A) Histograms indicate frequencies of *dC/dt* when worms commenced pirouette behaviours in each condition. (B) Slopes show cumulative probabilities of the frequencies in (A): left, single and population; middle, single and paired; right, population and paired. Each colour means as follows: blue, single; red, population; green, paired (N = 12, n = 93, 96 and 95 respectively; nonparametric two-sample Anderson-Darling test with Bonferroni correction; *$p < 0.05$, ***$p < 0.001$ significant difference; n.s., not significant, $p > 0.05$).

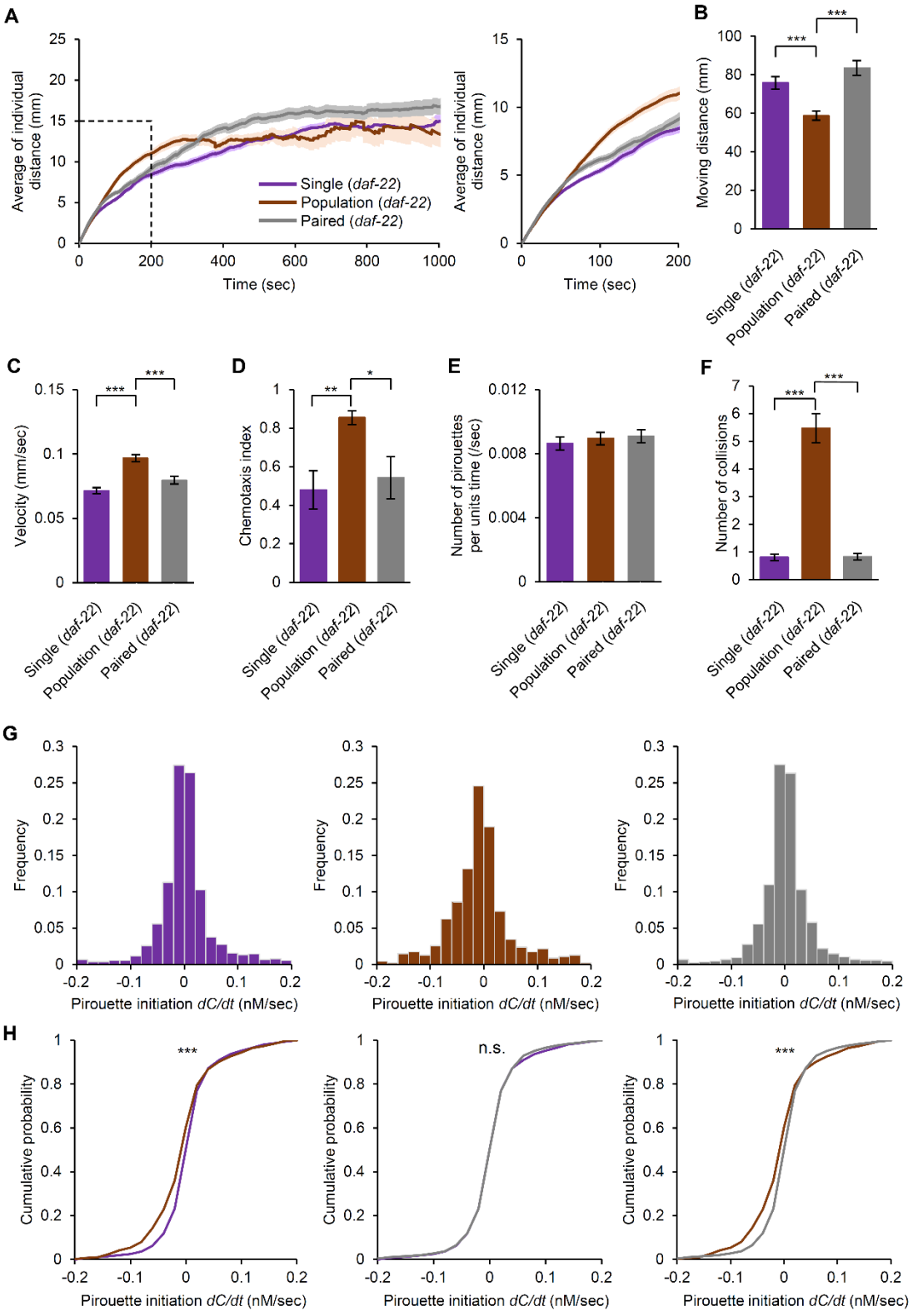

Fig. 3. Collective behaviour of the *daf-22* mutant in chemotaxis. (A) Average distances between individual worms. Each trace indicates the average distance between neighbouring worms. Shading in the graphs shows s.e.m. The right graph is an enlarged image of the dotted box in the left graph. (B-F) Mean of the moving distance (B), velocity (C), chemotaxis index (D), number of pirouettes per unit time (E), and number of collisions (F). Error bars indicate s.e.m. (G) Histograms indicate frequencies of dC/dt when *daf-22* commenced pirouette behaviours in each condition. (H) Slopes show cumulative probabilities of the frequencies in (G): left, single and population; middle, single and paired; right, population and paired. Purple, single condition; brown, population; grey, paired condition (N = 12, n = 90, 92 and 94 respectively; (B, E, F), Mann-Whitney *U* test with Bonferroni correction; (C, D), Student's *t*-test with Bonferroni correction; nonparametric two-sample Anderson-Darling test with Bonferroni correction; *$p < 0.05$, **$p < 0.01$, ***$p < 0.001$ significant difference; n.s., not significant, $p > 0.05$).

Supplemental Figures

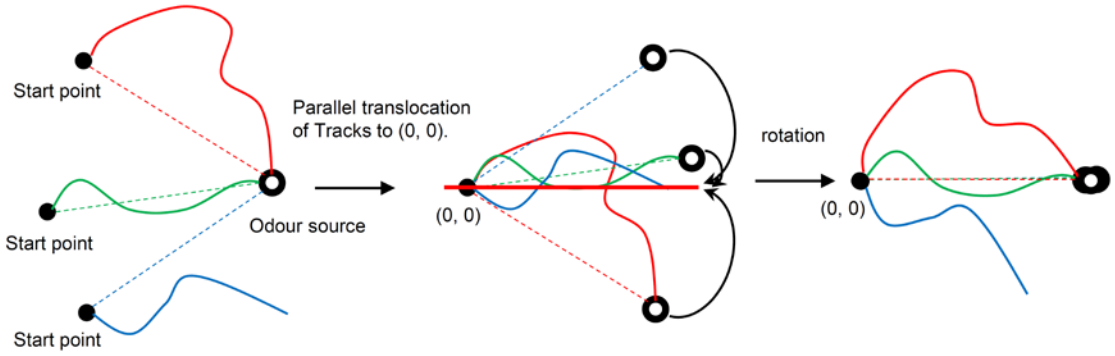

Fig. S1 Scheme of the pre-processing in analysis. To calculate the average distances between individual worms in the single and paired conditions, the trajectories were translocated and rotated in advance (the detail was described in materials and methods).

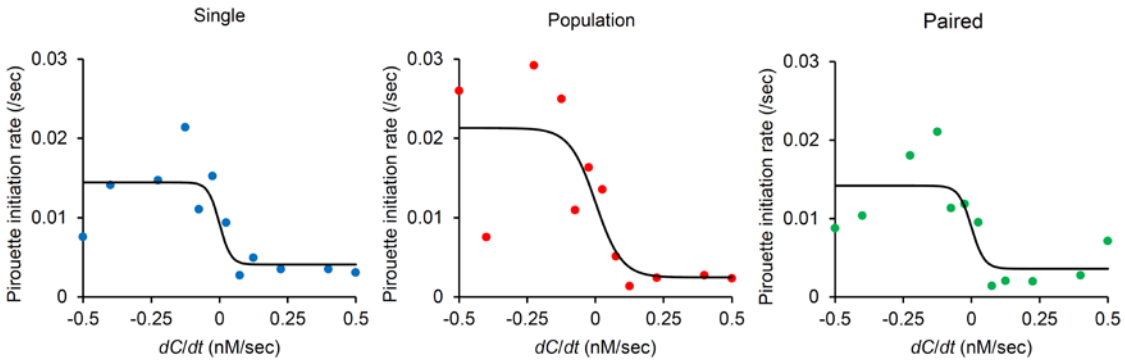

Fig. S2. Pirouette behaviours in each condition. The pirouette initiation rate plotted against *dC*/*dt*. Plots were fitted with a sigmoid curve (see materials and methods).

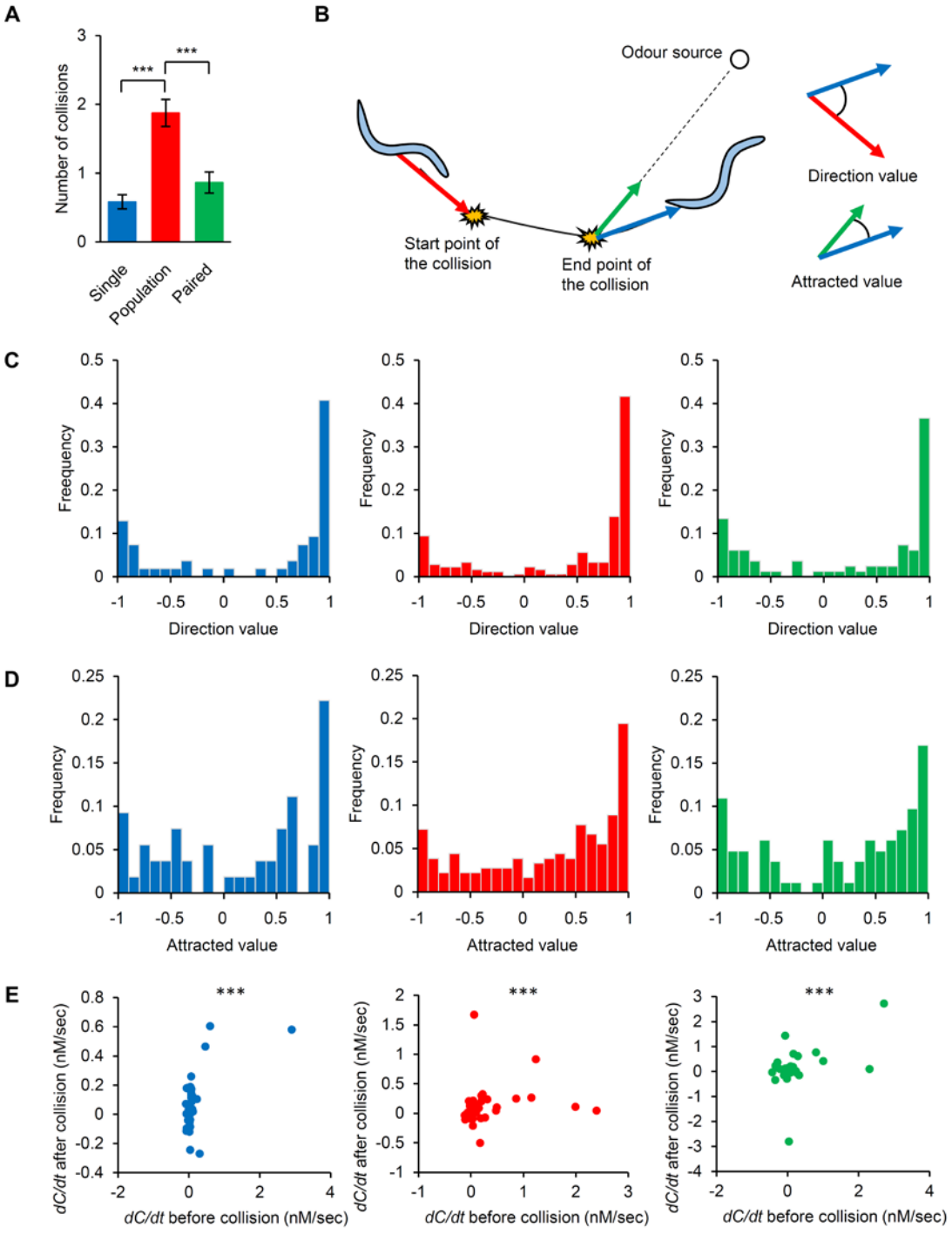

Fig. S3. Direction changes due to collisions of worms. (A) Mean number of collisions. Error bars indicate s.e.m. (B) The scheme of the direction and attracted value when worms collided others. The direction value reflects the cosine of the direction vector before and after collision. The attracted value

means the cosine of the direction vector after collision and the direction vector to the odour source. (C) Histograms of the direction values. (D) Histograms of the attracted values. (E) The relationship of *dC/dt* before and after contacts. The correlation coefficient was described in Table S1. Blue, single; red, population; green, paired. (N = 12, n = 93, 96 and 95, respectively; (A) Mann-Whitney *U* test with Bonferroni correction; (E) test for association/correlation between paired samples; ***p < 0.001, significant difference).

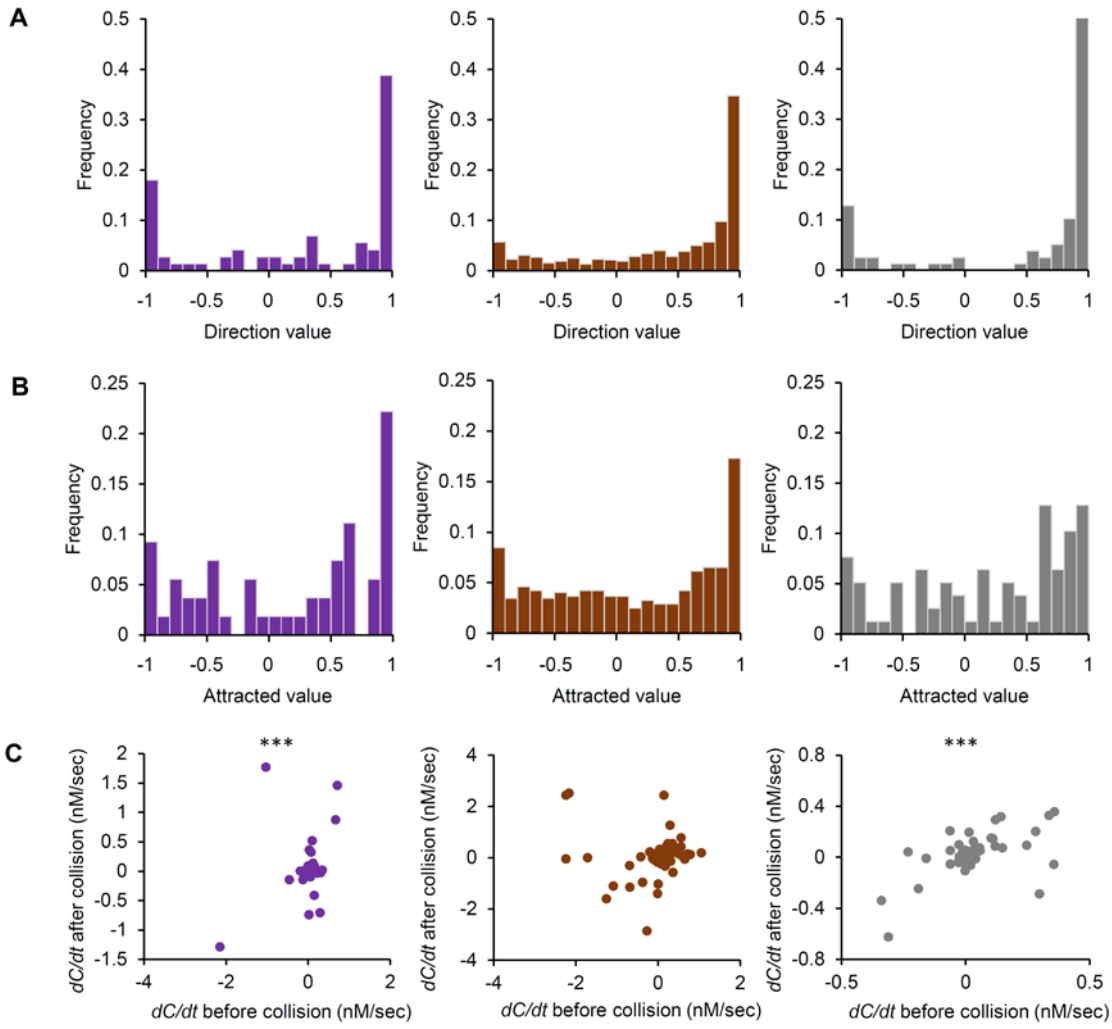

Fig. S4. Direction changes due to collisions of *daf-22* mutant. (A) Histograms of the direction values. (B) Histograms of the attracted values. (C) The relationship of *dC/dt* before and after contacts. The correlation coefficient was described in Table S1. Purple, single; brown, population; grey, paired. (N = 12, n = 90, 95 and 94, respectively; (C) test for association/correlation between paired samples; ***p < 0.001 significant difference).

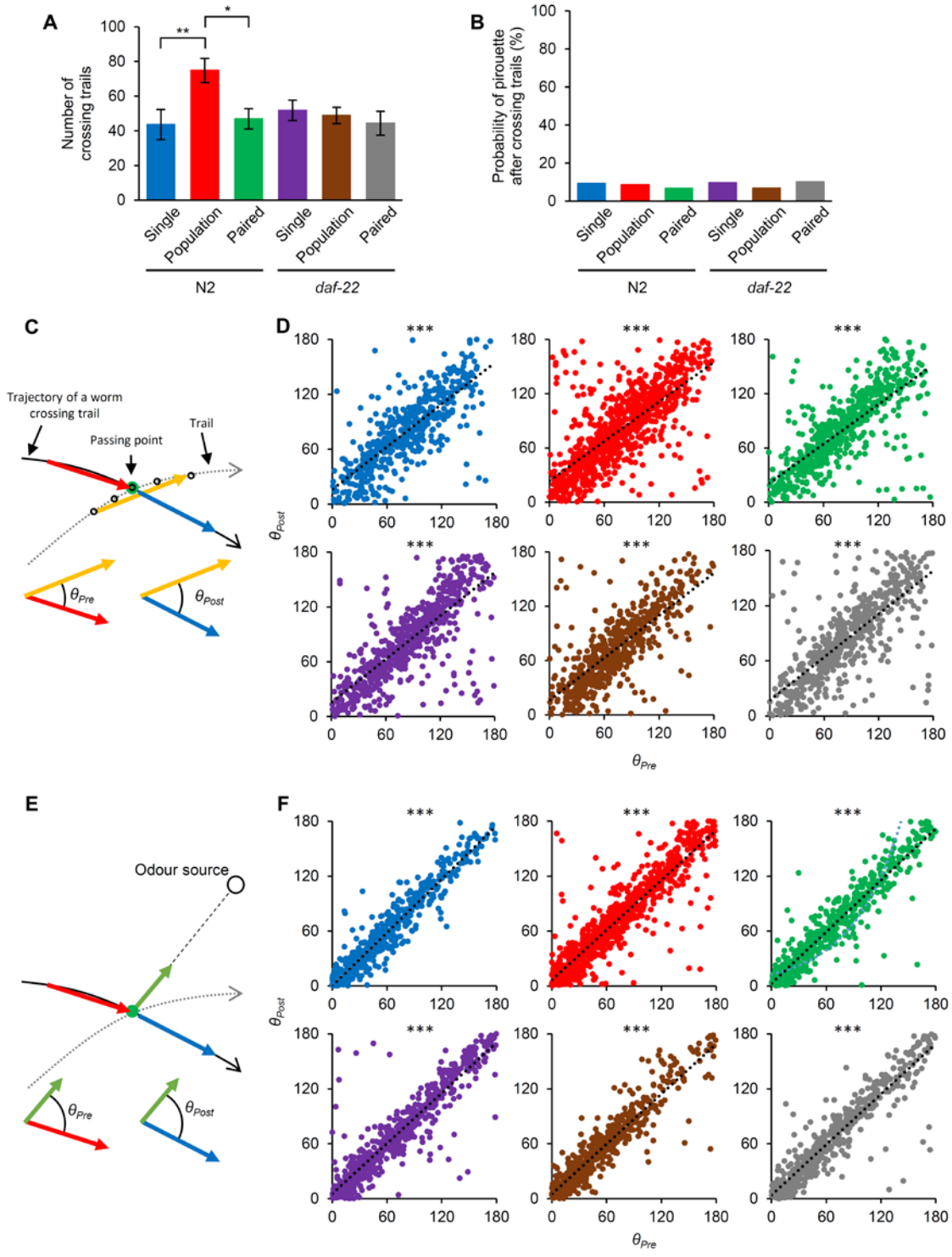

Fig. S5. Direction changes when worms crossed trails. (A) Mean of the number of crossing trails per an assay. The error bar indicates s.e.m (N = 12 in each condition). (B) Probability of pirouettes by 10 s after crossing trails. The probability is calculated as (the total number of pirouette by 10 s after

crossing trails) / (the total number of crossing trails). The values in all conditions were not significantly different from randomly sampled data (Table S2, see materials and methods). (C, D) Direction changes to trails. (C) Scheme of the direction changes to trails. (D) The relationship of angle before and after worms crossing trails. The correlation coefficient was described in Table S1. The slope of linear function was as follows: N2, single, 0.778, population, 0.727, paired, 0.728; *daf-22*, single, 0.793, population, 0.781, paired, 0.781) (E, F) Direction changes to odour source. (E) Scheme of the direction changes to odour source. (F) The relationship of angle to odour source before and after worms crossing trails. The correlation coefficient was described in Table S1. The slope of linear function was as follows: N2, single, 0.973, population, 0.908, paired, 0.939; *daf-22*, single, 0.916, population, 0.910, paired, 0.921. Blue, single; red, population; green, paired; purple, single (*daf-22*); brown, population (*daf-22*); grey, paired (*daf-22*) ((A) Mann-Whitney *U* test with Bonferroni correction; (B) binomial test; (E) test for association/correlation between paired samples; *p < 0.05, **p < 0.01, ***p < 0.01 significant difference).

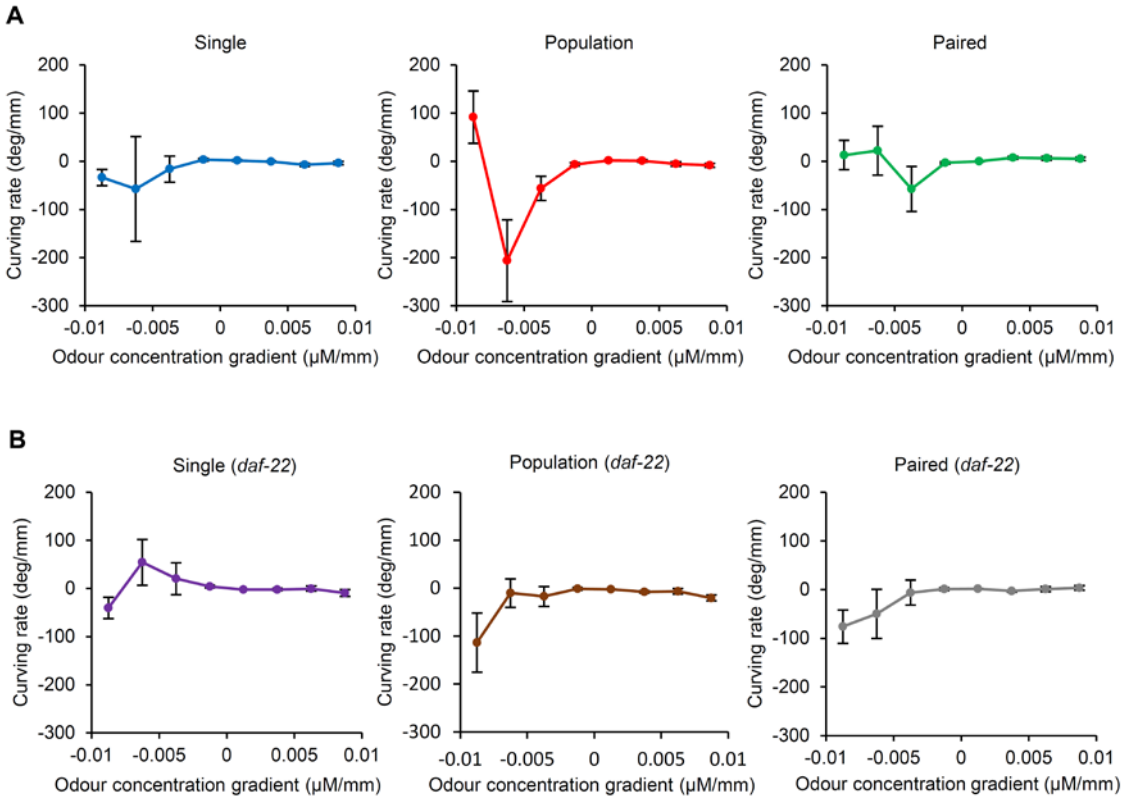

Fig. S6. Direction changes under collective conditions. (A, B) Curving rate against the normal odour gradient of N2 (A) and the *daf-22* mutant (B). Error bars indicate s.e.m. (N = 12, n = 93, 96, 95, 90, 95 and 94, respectively).

Table S1. Correlation coefficient and *p*-value of the results.

		N2			*daf-22*		
		Single	Population	Paired	Single	Population	Paired
Fig. S3E Fig. S4C	correlation coefficient	0.599	0.248	0.49	0.303	-0.0779	0.576
	p-value	1.69×10^{-6}	7.73×10^{-4}	3.04×10^{-6}	9.64×10^{-3}	0.0768	3.44×10^{-8}
Fig. S5D	correlation coefficient	0.789	0.721	0.739	0.773	0.753	0.752
	p-value	$<2.2 \times 10^{-16}$	$<2.2 \times 10^{-16}$	$<2.2 \times 10^{-16}$	$<2.2 \times 10^{-16}$	$<2.2 \times 10^{-16}$	$<2.2 \times 10^{-16}$
Fig. S5F	correlation coefficient	0.953	0.912	0.938	0.915	0.933	0.928
	p-value	$<2.2 \times 10^{-16}$	$<2.2 \times 10^{-16}$	$<2.2 \times 10^{-16}$	$<2.2 \times 10^{-16}$	$<2.2 \times 10^{-16}$	$<2.2 \times 10^{-16}$

Table S2. Parameters for binominal test used in Fig. S6

	N2			*daf-22*		
	Single	Population	Paired	Single	Population	Paired
number of passing points	524	898	563	621	586	533
number of pirouette by 10 s after worms crossed trails	49	78	38	60	40	54
hypothesized probability of pirouette	0.0876	0.104	0.0707	0.0876	0.0853	0.0944
p-value	0.642	0.09	0.869	0.434	0.159	0.554

Supplemental Figures

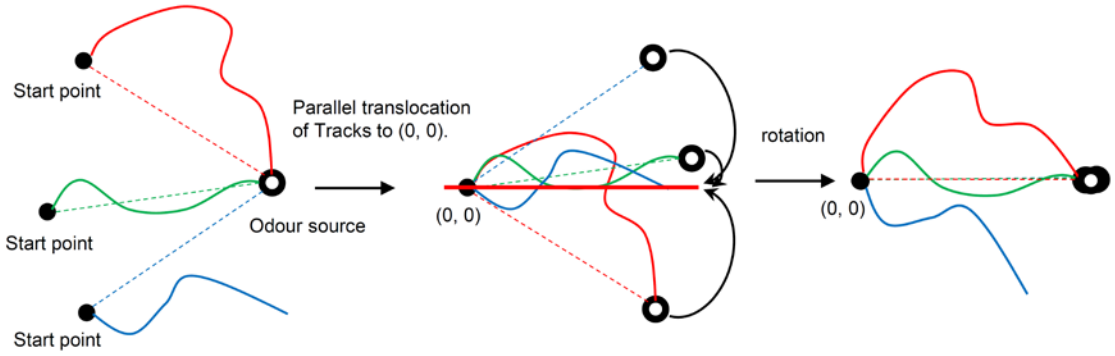

Fig. S1 Scheme of the pre-processing in analysis. To calculate the mean distances between individual worms in the single and paired conditions, the trajectories were translocated and rotated in advance (the detail was described in materials and methods).

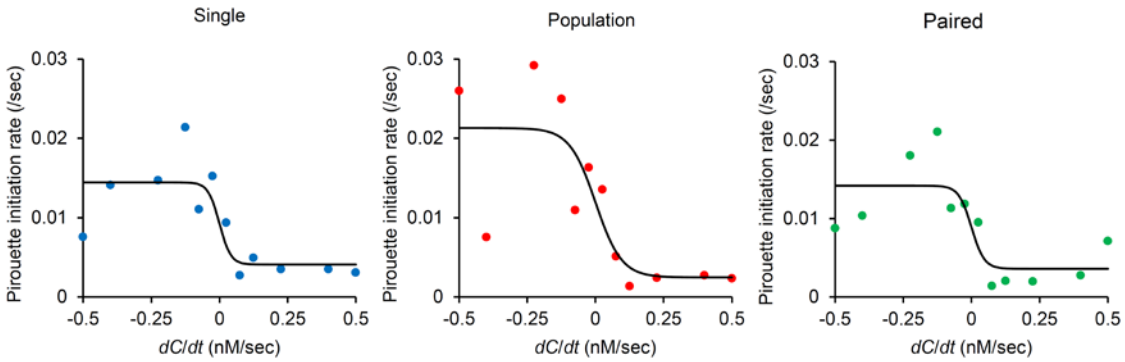

Fig. S2. Pirouette behaviours in each condition. The pirouette initiation rate plotted against d*C*/d*t*. Plots were fitted with a sigmoid curve (see materials and methods).

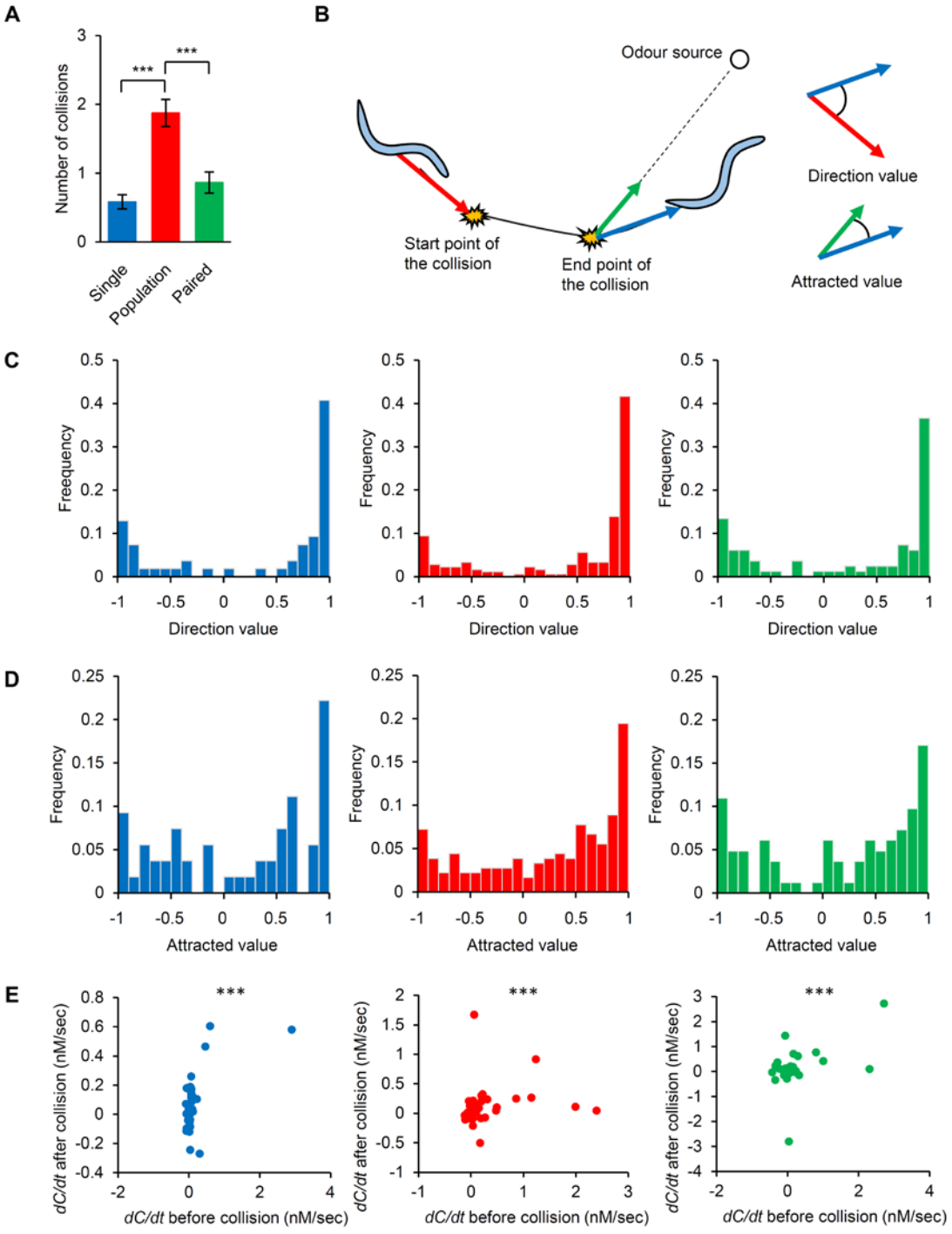

Fig. S3. Direction changes due to collisions of worms. (A) Mean (±s.e.m.) number of collisions. (B) Scheme of the direction and attracted value when worms collided with others. The direction value reflects the cosine of the direction vector before and after collision. The attracted value

means the cosine of the direction vector after collision and the direction vector to the odour source. (C) Histograms of the direction values. (D) Histograms of the attracted values. (E) The relationship of d*C*/d*t* before and after contacts. The correlation coefficient was described in Table S1 ($N = 12$, $n = 93$, 96 and 95, respectively, for single, population, paired). A: Mann-Whitney *U* test with Bonferroni correction; E: test for association/correlation between paired samples; ***$P<0.001$, significant difference.

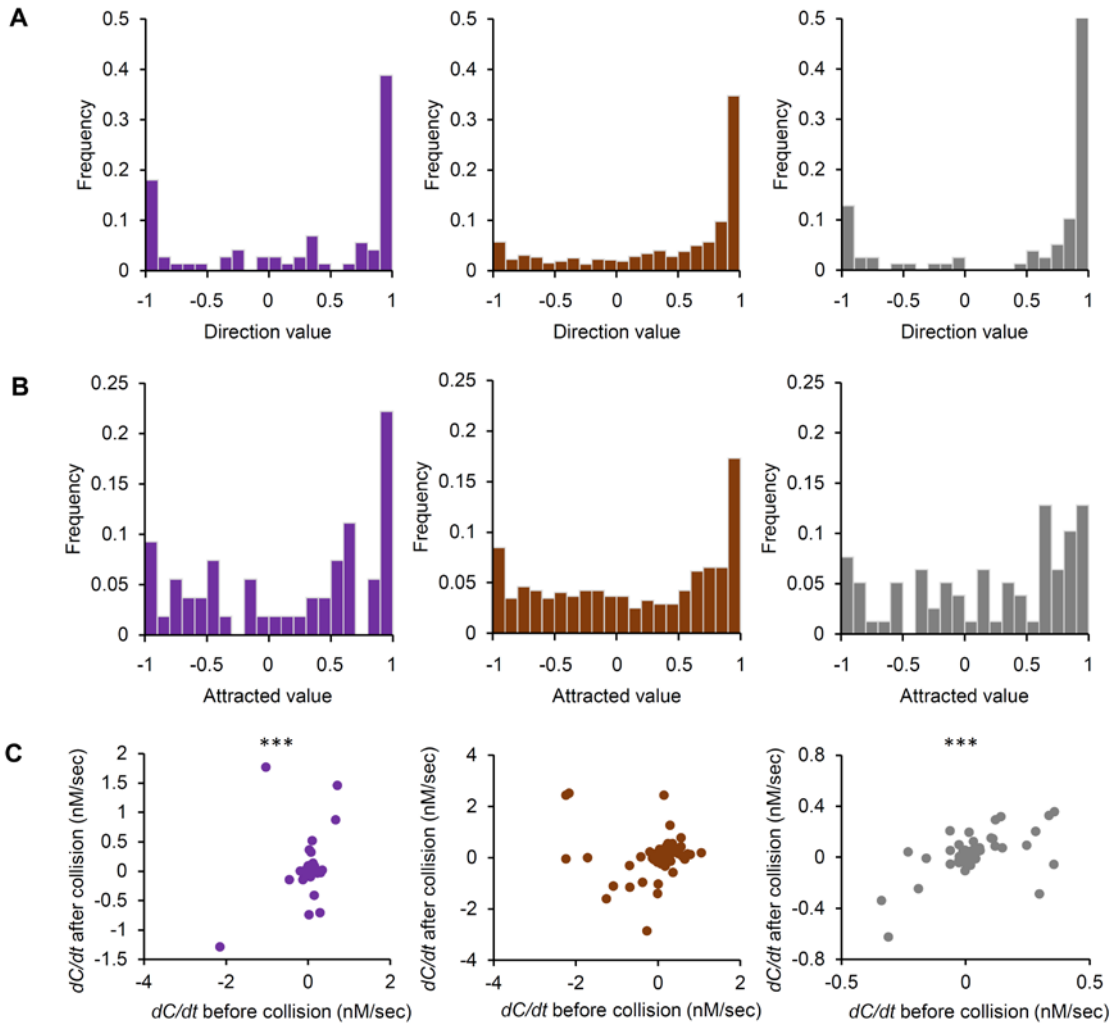

Fig. S4. Direction changes due to collisions of *daf-22* mutant. (A) Histograms of the direction values. (B) Histograms of the attracted values. (C) The relationship of d*C*/d*t* before and after contacts. The correlation coefficient was described in Table S1 [N = 12, n = 90, 95 and 94, respectively, for single (purple), population (brown), paired (grey)]. C: test for association/correlation between paired samples; ****P*<0.001 significant difference.

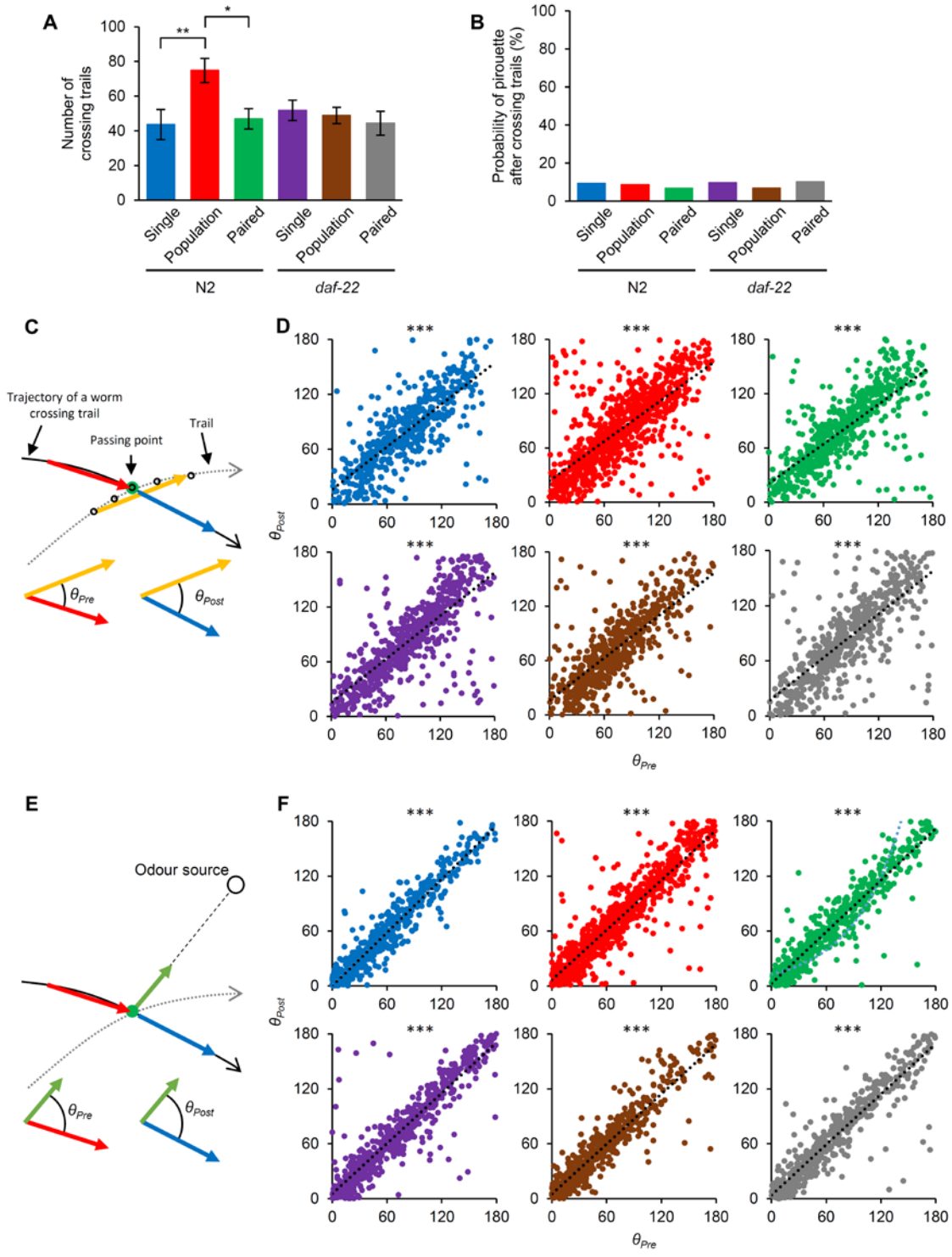

Fig. S5. Direction changes when worms crossed trails. (A) Mean (±s.e.m) of the number of crossing trails per an assay (N = 12 in each condition). (B) Probability of pirouettes by 10 s after crossing trails. The probability is calculated as (the total number of pirouette by 10 s after

crossing trails) / (the total number of crossing trails). The values in all conditions were not significantly different from randomly sampled data (Table S2, see materials and methods). (C, D) Direction changes to trails. (C) Scheme of the direction changes to trails. (D) The relationship of angle before and after worms crossing trails. The correlation coefficient was described in Table S1. The slope of linear function was as follows: N2, single (blue), 0.778, population (red), 0.727, paired (green), 0.728; *daf-22*, single (purple), 0.793, population (brown), 0.781, paired (grey), 0.781. (E, F) Direction changes to odour source. (E) Scheme of the direction changes to odour source. (F) The relationship of angle to odour source before and after worms crossing trails. The correlation coefficient was described in Table S1. The slope of linear function was as follows: N2, single, 0.973, population, 0.908, paired, 0.939; *daf-22*, single, 0.916, population, 0.910, paired, 0.921. A: Mann-Whitney *U* test with Bonferroni correction; B: binomial test; E: test for association/correlation between paired samples; **P*<0.05, ***P*<0.01, ****P*<0.001 significant difference.

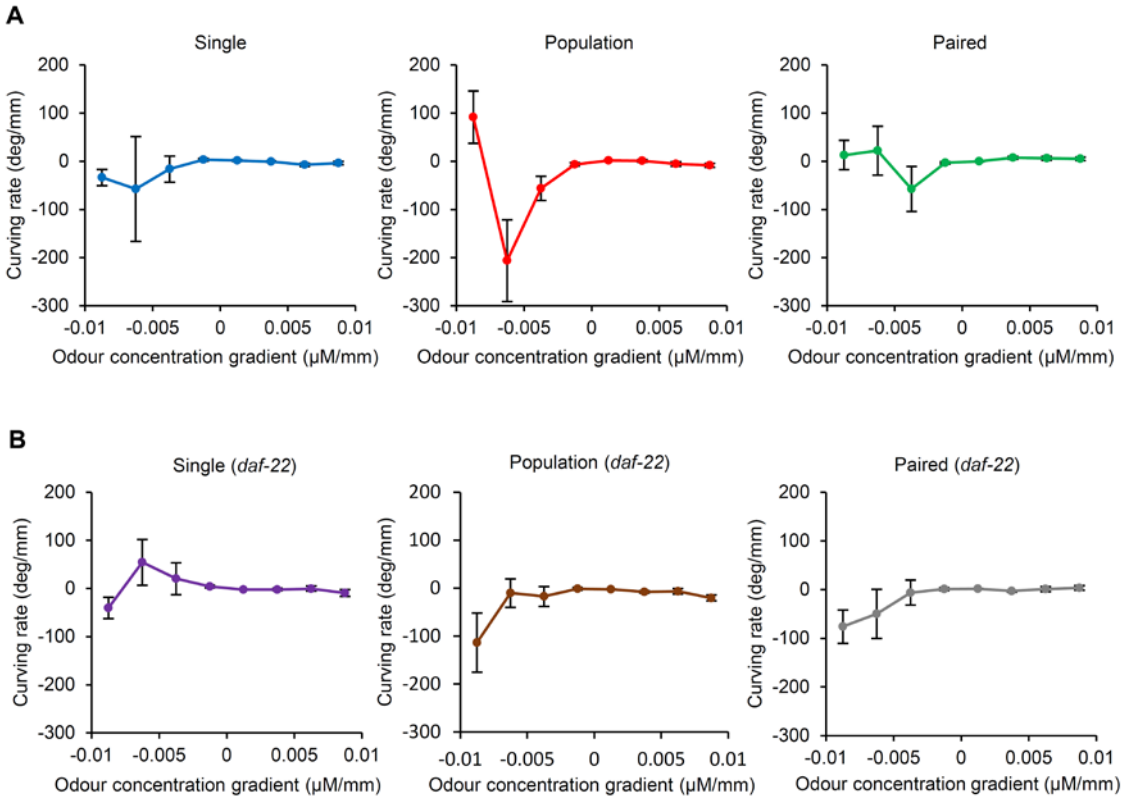

Fig. S6. Direction changes under collective conditions. (A, B) Curving rate (±s.e.m.) against the normal odour gradient of N2 (A) and the *daf-22* mutant (N = 12, n = 93, 96, 95, 90, 95 and 94, respectively).

Table S1. Correlation coefficient and *p*-value of the results.

		N2			*daf-22*		
		Single	Population	Paired	Single	Population	Paired
Fig. S3E Fig. S4C	correlation coefficient	0.599	0.248	0.49	0.303	-0.0779	0.576
	p-value	1.69×10^{-6}	7.73×10^{-4}	3.04×10^{-6}	9.64×10^{-3}	0.0768	3.44×10^{-8}
Fig. S5D	correlation coefficient	0.789	0.721	0.739	0.773	0.753	0.752
	p-value	$<2.2 \times 10^{-16}$	$<2.2 \times 10^{-16}$	$<2.2 \times 10^{-16}$	$<2.2 \times 10^{-16}$	$<2.2 \times 10^{-16}$	$<2.2 \times 10^{-16}$
Fig. S5F	correlation coefficient	0.953	0.912	0.938	0.915	0.933	0.928
	p-value	$<2.2 \times 10^{-16}$	$<2.2 \times 10^{-16}$	$<2.2 \times 10^{-16}$	$<2.2 \times 10^{-16}$	$<2.2 \times 10^{-16}$	$<2.2 \times 10^{-16}$

Table S2. Parameters for binominal test used in Fig. S6

	N2			*daf-22*		
	Single	Population	Paired	Single	Population	Paired
number of passing points	524	898	563	621	586	533
number of pirouette by 10 s after worms crossed trails	49	78	38	60	40	54
hypothesized probability of pirouette	0.0876	0.104	0.0707	0.0876	0.0853	0.0944
p-value	0.642	0.09	0.869	0.434	0.159	0.554